Three-dimensional assessment of brain tissue morphology

Bert Müller*[a], Marco Germann[a,b], Daniel Jeanmonod[b], Anne Morel[b]
[a]Computer Vision Laboratory ETH Zürich, Sternwartstrasse 7, 8092 Zürich, SWITZERLAND;
[b]Department of Functional Neurosurgery, University Hospital Zurich, Sternwartstrasse 6, 8091 Zürich, SWITZERLAND
*present address: Medical Faculty, University of Basel, Schanzenstrasse 46, 4031 Basel, SWITZERLAND

ABSTRACT

The microstructure of brain tissues becomes visible using different types of optical microscopy after the tissue sectioning. This preparation procedure introduces stress and strain in the anisotropic and inhomogeneous soft tissue slices, which are several 10 µm thick. Consequently, the three-dimensional dataset, generated out of the two-dimensional images with lateral sub-micrometer resolution, needs algorithms to correct the deformations, which can be significant for mellow tissue such as brain segments. The spatial resolution perpendicular to the slices is much worse with respect to the lateral sub-micrometer resolution. Therefore, we propose as complementary method the synchrotron-radiation-based micro computed tomography (SRµCT), which avoids any kind of preparation artifacts due to sectioning and histological processing and yields true micrometer resolution in the three orthogonal directions. The visualization of soft matter by the use of SRµCT, however, is often based on elaborate staining protocols, since the tissue exhibits (almost) the same x-ray absorption as the surrounding medium. Therefore, it is unexpected that human tissue from the pons and the medulla oblongata in phosphate buffer show several features such as the blood vessels and the inferior olivary nucleus without staining. The value of these tomograms lies especially in the precise non-rigid registration of the different sets of histological slices. Applications of this method to larger pieces of brain tissue, such as the human thalamus are planned in the context of stereotactic functional neurosurgery.

Keywords: Imaging techniques, micro computed tomography, brain tissue, blood vessels, registration

1. INTRODUCTION

The execution of stereotactic functional neurosurgery without penetration and physiological control requires the precise determination of the targeted lesion position solely based on magnetic resonance imaging. The location of the target, e.g. in the thalamus, with desired precision is possible, even if the targeted nuclei are invisible on the acquired images using the atlas of the human thalamus.[1,2] The application of the atlas and prior knowledge to the actual therapy is, however, a specific process. The current planning of the intervention, basically relying on fixed spatial relations between target areas and pre-defined anatomical landmarks can be significantly improved and generalized by taking into account the full variability of the underlying anatomical structures. One of the open issues is the establishment of anatomically meaningful correspondence between the individual structures in the training set, which is still subject of ongoing research.[3,4] Due to the very high complexity of the related model, the establishment of correspondence between stained histological slices belongs to the major challenges when trying to build a corresponding statistical shape model. Suitable algorithms allow fitting the average model to the actual patient using only structural data available from magnetic resonance imaging.

Structure and morphology of human tissues, as for the generic brain atlas, are generally characterized on sub-micrometer level using optical microscopy, preparing parallel histological slices several 10 µm thick. The stress and strain introduced by the preparation procedure leads to deformations of the anisotropic and inhomogeneous soft matter, expected to be especially critical for mellow tissue such as brain segments. In order to get the true 3D representation, the deformations have to be corrected visualizing and quantifying the anatomic features of the tissue.

*bert.mueller@unibas.ch; phone +41 44 6336190

Developments in X-Ray Tomography V, edited by Ulrich Bonse,
Proc. of SPIE Vol. 6318, 631803, (2006) · 1605-7422/06/$15 · doi: 10.1117/12.680312

Synchrotron-radiation-based micro computed tomography (SRμCT) provides the necessary spatial and, to some extend, also density resolution, as shown by preliminary results of rather small pieces of brain tissue in 2005.[5] Even without any staining, several anatomical features are uncovered in the individual SRμCT-slices. For example, one can clearly identify the inferior olivary nucleus, which is an agglomeration of neuronal cells and which exhibits higher absorption than the surrounding tissue. Fiber tracts are also visible in the tomogram. Holes with diameters of several 10 μm in the histological slices are attributed to the larger blood vessels. Many blood vessels seem to be collapsed in the 3D configuration and presumably originate significant distortions in the histological slices. The value of the tomogram, therefore, lies in particular in the possibility to non-rigidly register the different sets of histological slices by means of the available, less-detailed 3D data. The combination of the different information at the micrometer and millimeter scales offers a promising tool to significantly improve the generic brain atlas and thereby the minimally invasive or even non-invasive patient treatment using facilities such as focused 3D ultrasound under magnetic resonance guidance.

The following tasks have to be carried out to reach the envisioned target. First, the conversion of the current slice-based atlas data into a fully 3D representation, based on a dense set of points in an anatomically defined coordinate system incorporating the information of SRμCT. Second, the establishment of reasonable correspondence between the individual anatomies. This procedure will be based on interactive definition of visible landmark structures, followed by automatic adjustment to reach dense correspondence relations. Third, the training of an average model and the de-correlated set of shape variation modes by principle component analysis. Finally, the implementation of optimization algorithms fitting the average model to the actual patient data while respecting the pre-determined modes of variation resulting from the previous training step must be accomplished. This fitting procedure will only use structural data available from the magnetic resonance imaging acquisition overlaying the full set of mostly invisible, relevant nuclei onto the radiological images.

Consequently, the currently available brain atlas (Morel atlas)[1] will could be improved, first by extending the underlying histological data by SRμCT, second by investigating the possibility to include tomographic datasets with only partially defined structures, third systematically quantifying the precision of the structural prediction of the statistical atlas and the necessity to incorporate further datasets into the model, and finally by investigating the use of appearance-based predictors from the magnetic resonance images to improve the fitting process.

2. SRμCT MEASUREMENTS

Synchrotron-radiation-based micro computed tomography (SRμCT) in absorption contrast mode is well established to quantitatively characterize the three-dimensional (3D) morphology of different kinds of biomaterials and the anatomy of various human tissues with true micrometer resolution. The main advantage with respect to conventional μCT is the much higher photon flux, offering to eliminate all x-ray photons but the ones of selected energy, and still maintain a reasonable acquisition time. Bragg reflection at single crystals permits the selection of the photon energy with the precision of 10^{-4}. Consequently, synchrotron radiation became a tuneable x-ray source also for tomographic imaging. Because the x-ray absorption coefficient μ strongly depends on both energy E and atomic number Z, the choice of the photon energy can be optimized minimizing the total exposure time at any prescribed sensitivity by the relation $\mu(E,Z) \cdot D = 2$, where D corresponds to the average sample diameter, as shown by Grodzins.[6] Accordingly; we selected the photon energy of 10 keV for the present study. The spatial resolution was determined by the modulation transfer function of an edge of a gold plate recorded under the conditions applied for the data acquisition[7] and corresponds to 6.20 and 4.25 μm for the brain segments in formalin/phosphate buffer and in paraffin, respectively. Note, the voxel lengths were chosen to 4.05 and 2.10 μm because of the different specimen diameters.

The experiments were carried out at the beamline BW 2 (HASYLAB at DESY) taking advantage of the standard setup for tomography.[8] Positrons with the energy of 4.5 GeV are forced to travel along a curved path by the bending magnets of the storage ring DORIS III. The wiggler of the beamline BW 2 is a magnetic structure of 28 periods to generate the necessary photon flux. The fixed exit double crystal monochromator, Si(111) provides the monochromatic x-ray beam of desired energy and flux. The sagitally bent second Si(111) crystal reduces the beam divergence and forms a parallel beam about 10 mm wide and 3 mm high. This beam hits the sample at a certain angle and generates the related projection image on the fluorescence screen, which was a 1000 μm-thick $CdWO_4$ single crystal. After moderate magnification this optical image is mapped on a Kodak KAF 1600 CCD-chip (1536 x 1024 pixels, pixel length 9 μm) and acquired using 14 bit digitalization at a frequency of 1.25 MHz. The sample manipulator allows the precise specimen positioning and rotation. For the present study, 4 datasets at different sample heights (shifted by 1.5 mm) each with 721 projections were acquired by rotating the sample in steps of 0.25° from 0 to 180°. In order to eliminate the beam non-uniformities and account for the detector noise, the difference between the individual bare projections and the dark image was divided by the difference of the beam and the dark image to obtain the

corrected projections, which were the basis of the reconstruction. Nevertheless, image inhomogeneities still existed due to the photon counting statistics and non-uniformities and defects in the fluorescence screen. The reconstruction was performed slice-by-slice with the filtered back projection algorithm.[9] In order to improve the density resolution,[10] the data were also binned by the factors of 2, 3, and 4 before reconstruction. For the 3D visualization of the blood vessel system the software VG Studio Max (Volume Graphics, Heidelberg, Germany) was applied.

3. BRAIN TISSUE SELECTIONS AND PREPARATION

The brain tissue consists of neuronal cells, axons and glial. In neurosurgery, special interest is in the arrangements of neuronal cells, which form nuclei and fiber tracts, which may exhibit stronger or lower absorption than the surrounding tissue.

Many descriptions of the brain anatomy are known. As shown in Fig. 1, we just discriminate here between the forebrain (blue colored), the midbrain (green colored), and the hindbrain (yellow colored). For the experiments, parts of the pons and the medulla were selected. This tissue was conserved in formalin for about 12 months. After cutting into pieces of appropriate size, it was transferred to 0.5 ml Eppendorf tubes and entirely filled with phosphate buffer (PB). Alternatively, other pieces were embedded into paraffin, which is known to absorb x-rays less than water. Thus, the images should exhibit better contrast and the structures of interest should be segmented easier.

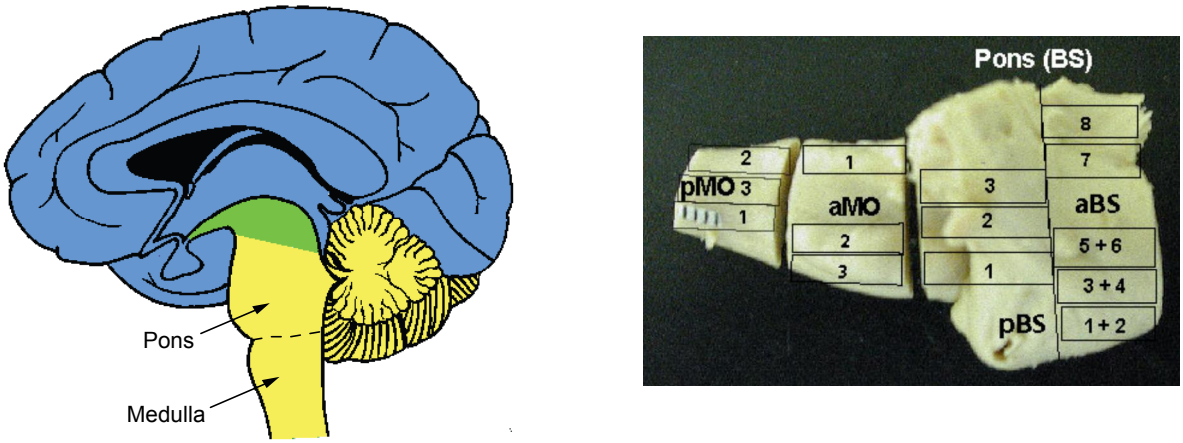

Fig. 1. The anatomy of the brain (left side) with forebrain (blue colored), midbrain (green colored), hindbrain (yellow colored). The locations of the selected pieces in the postmortem hindbrain are shown on the right. The results of the part of the medulla oblongata, termed pMO 3 and aMO 1 are illustrated below.

4. HISTOLOGICAL SECTIONING OF BRAIN TISSUE

Subsequent to the SRμCT measurements the specimens were investigated by means of histology. The specimens were embedded in paraffin or frozen for cryogenic cutting. The slices obtained were 10 μm thick for the paraffin embedding and 30 μm thick for the frozen sections. The thickness of the individual sections was not experimentally verified.

With respect to the paraffin embedded slices, the frozen sections are preferred, because these free-floating sections undergo less shrinkage[11] and multiple staining procedures are applicable.

The optical microscopy in bright- and dark-field mode provides images of the slices with high lateral spatial resolution. Depending on the staining performed, a variety of features can be more or less easily identified and quantitatively analyzed. Fig. 2 shows typical images of the Nissl stained tissue slices each 4 mm x 4 mm both in bright- (left) and dark-field (right) mode. The anatomical features of the medulla oblongata include the inferior olivary nucleus (ION), the pyramid (corticospinal

tract) and the medial lemniscus, which reflect, on the cellular level, neuronal cells (nerve fibers and cell bodies) as well as blood vessels.

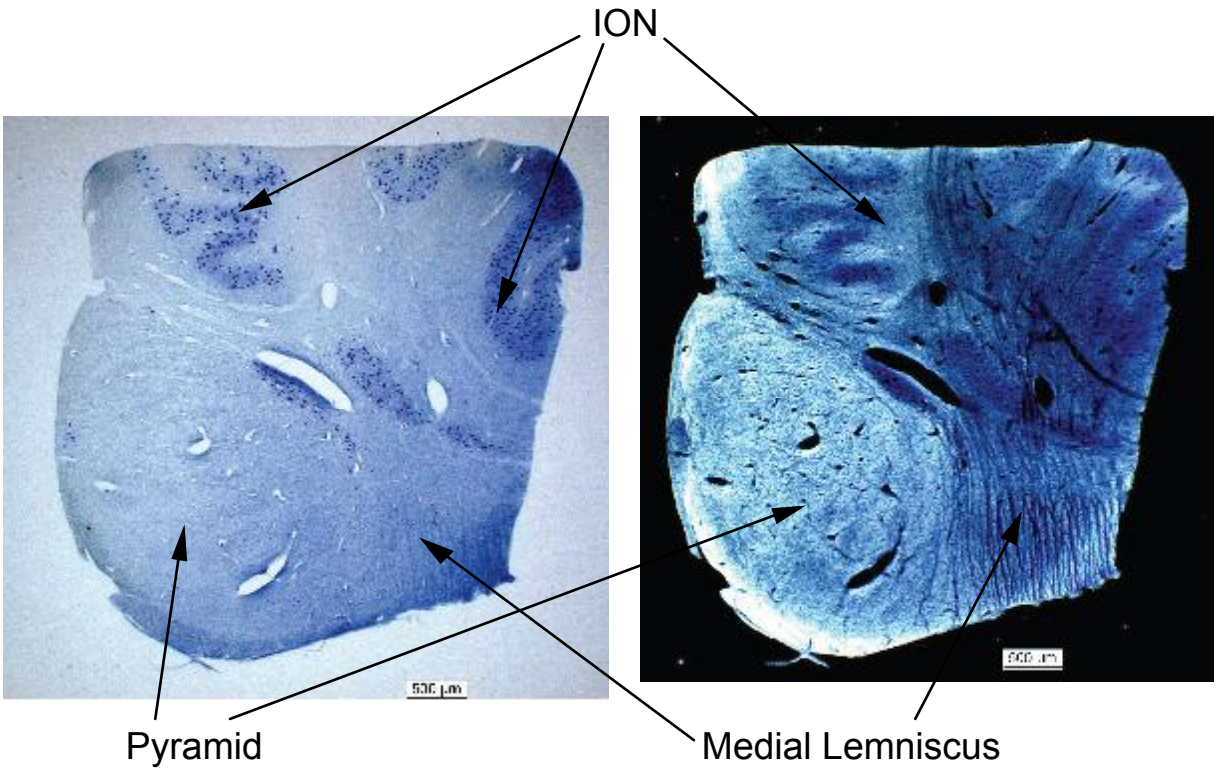

Fig. 2. Slices of brain tissue stained with Nissl – bright field (left) and dark field (right) – show the anatomical features of the medulla oblongata, including the inferior olivary nucleus (ION), nerve fibers, and cavities (blood vessels).

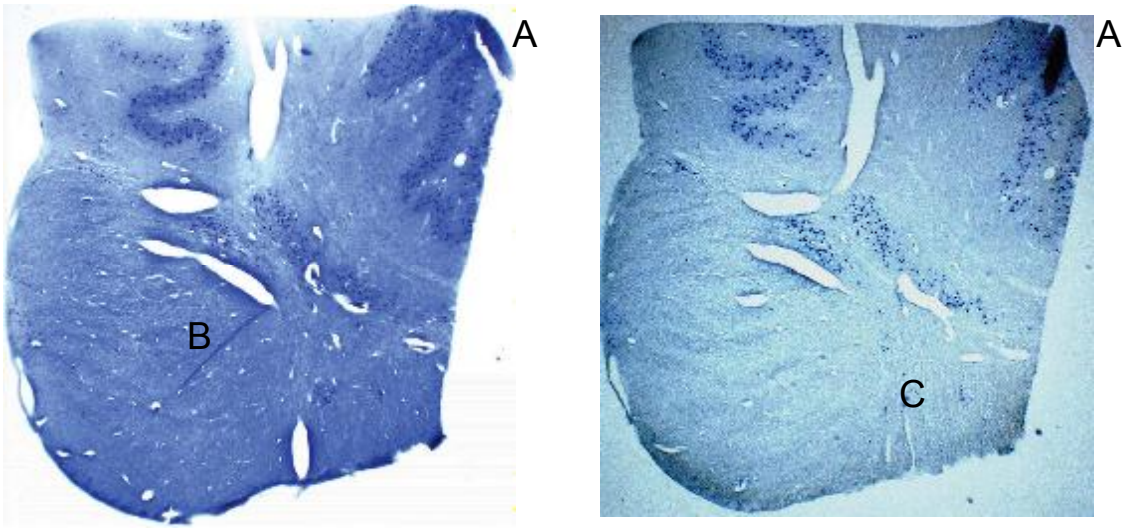

Fig. 3. Two subsequent histological slices of the medulla oblongata, which show some problems for automated registration resulting from illumination issues, artifacts such as folds (A), overlaps (B) and collapsed cavities (C) as well as changes due to the limited resolution in the third direction.

In order to obtain a 3D representation of the tissue, one has to combine the slices in the suitable manner. How difficult the task is, is shown in Fig. 3. Here, two subsequent slices are given, which reveal the problems in automated registration resulting from the differences in illumination (i.e. contrast), folds (A), overlaps (B), collapsed cavities (C) and major changes resulting from the limited resolution in the third direction. The power of histology, however, lies in the application of different staining protocols, which allows uncovering the detailed functionality of the cellular structures. Two examples, i.e. myelin and Nissl, are given in the present paper.

5. SRμCT OF PARAFFIN EMBEDDED BRAIN TISSUE

The blood vessel system of brain tissue should yield prominent anatomical landmarks for the registration of the 2D optical images of the histological slices. Paraffin embedding is expected to lead to better contrasting of the cavities than the measurements in water (phosphate buffer). Indeed, the SRμCT slices, represented in Fig. 4, exhibit clear contrast between air – represented in black, paraffin – represented in gray, and brain tissue – represented by the bright color. Several cavities are only partly or even not filled by paraffin. This effect simplifies the segmentation of the cavities. The tissue shows some internal structure, which well elucidates the anisotropy of the specimen.

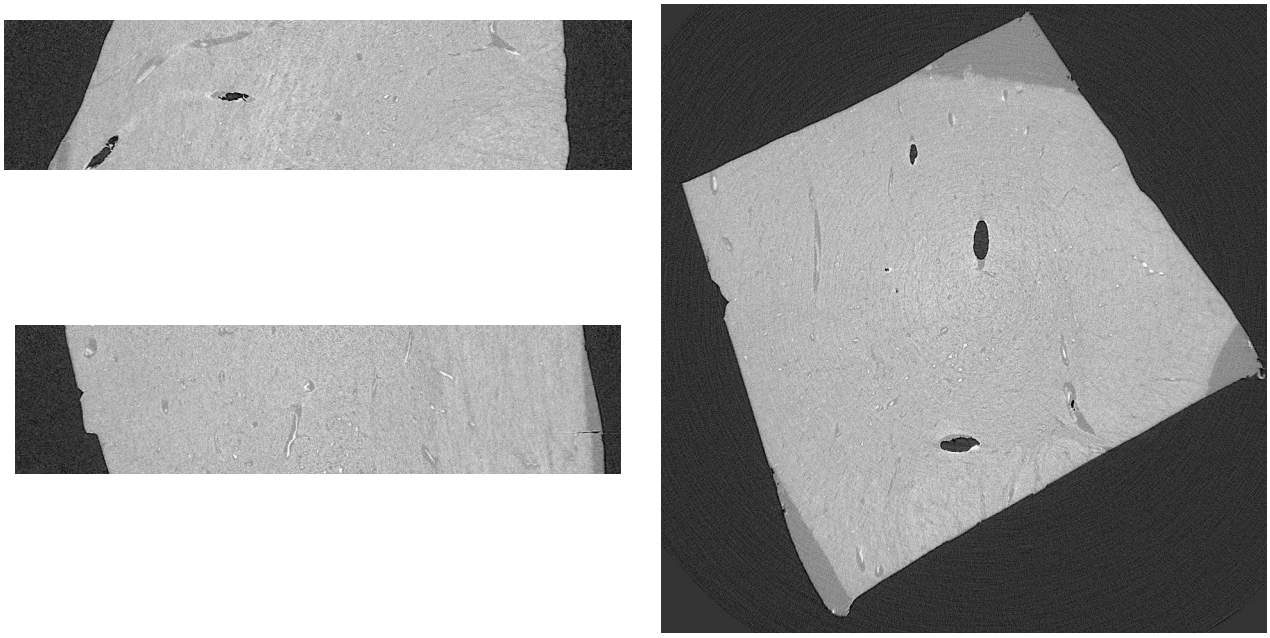

Fig. 4. The 3 orthogonal slices of paraffin embedded brain tissue are visualized by SRμCT and clearly allow segmenting tissue (bright), paraffin (gray) and air (black). Some cavities are not filled by paraffin. The anisotropic tissue structure is well represented.

Another phenomenon is shown in Fig. 5. The slice on the left clearly indicates that the cavities are surrounded by some stronger absorbing layer associated with the blood vessel walls, which further simplifies the intensity-based segmentation of the vessel tree. On the right of Fig. 5 a 3D representation of the segmented cavities is reproduced. Therefore, one can conclude that the segmented blood vessel system offers a route for the registration of the histological slices in the case of the paraffin embedded specimens.

It should be noted that even the smallest blood vessels, i.e. the capillaries are uncovered, because the voxel size corresponds to about 2 μm and the spatial resolution of 4 μm is equal or smaller than the diameters of the capillaries.

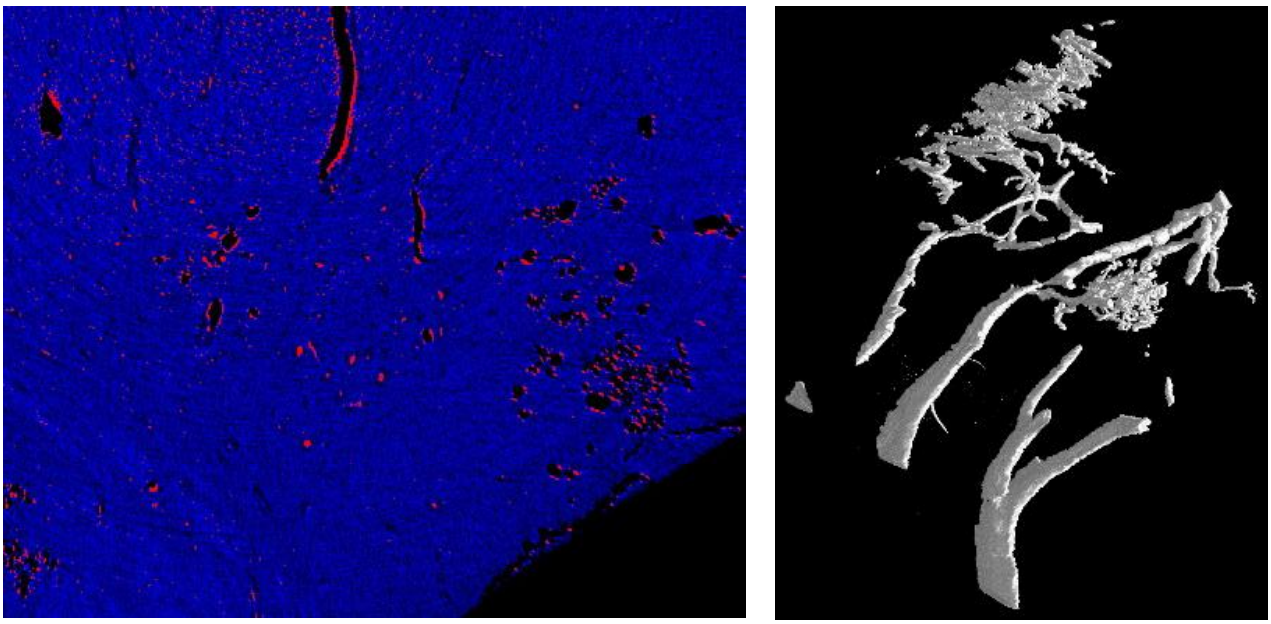

Fig. 5. The cavities (blood vessels) are surrounded by stronger absorbing species (cp. slice left). The blood vessel system can be extracted and visualized in 3D using intensity-based segmentation (right).

6. SRμCT OF BRAIN TISSUE IN WATER

Compared to the paraffin embedded specimens it is much more challenging to extract anatomical features of tissue in water, since the tissue consists mainly of water and thus the difference in absorption contrast is extremely weak. Nevertheless, we were able to make visible several landmarks as illustrated in Fig. 6. For imaging the data are binned by a factor of 3 prior to the reconstruction, which significantly enhances the density resolution or contrast reducing the spatial resolution.[10] In general, the tissue exhibits about 10% less absorption than the surrounding phosphate buffer. Therefore, the outer shape of the tissue is easily recorded. This helps to register the 2D optical slices. In our experiment, however, the tissue was in stronger contact with the wall of the Eppendorf container to avoid any undesired relative movement of the tissue during the necessary specimen rotation. Therefore, the outer shape of the optical slices and the SRμCT cannot be compared one-by-one.

The nuclei, which are identified by means of the histological slices, have in average a comparable absorption than the phosphate buffer. A closer look reveals a difference in x-ray absorption at the photon energy of 10 keV, which corresponds to around 1% using a binning factor of 3. The agglomeration of the neuronal cells can be segmented from the other kinds of tissue.

The fiber bundles are also seen, but the segmentation is difficult to perform.

In summary, the registration of the 2D optical slices can be performed best taking advantage of the segmentation and registration of the nuclei well extractable from both kinds of modalities.

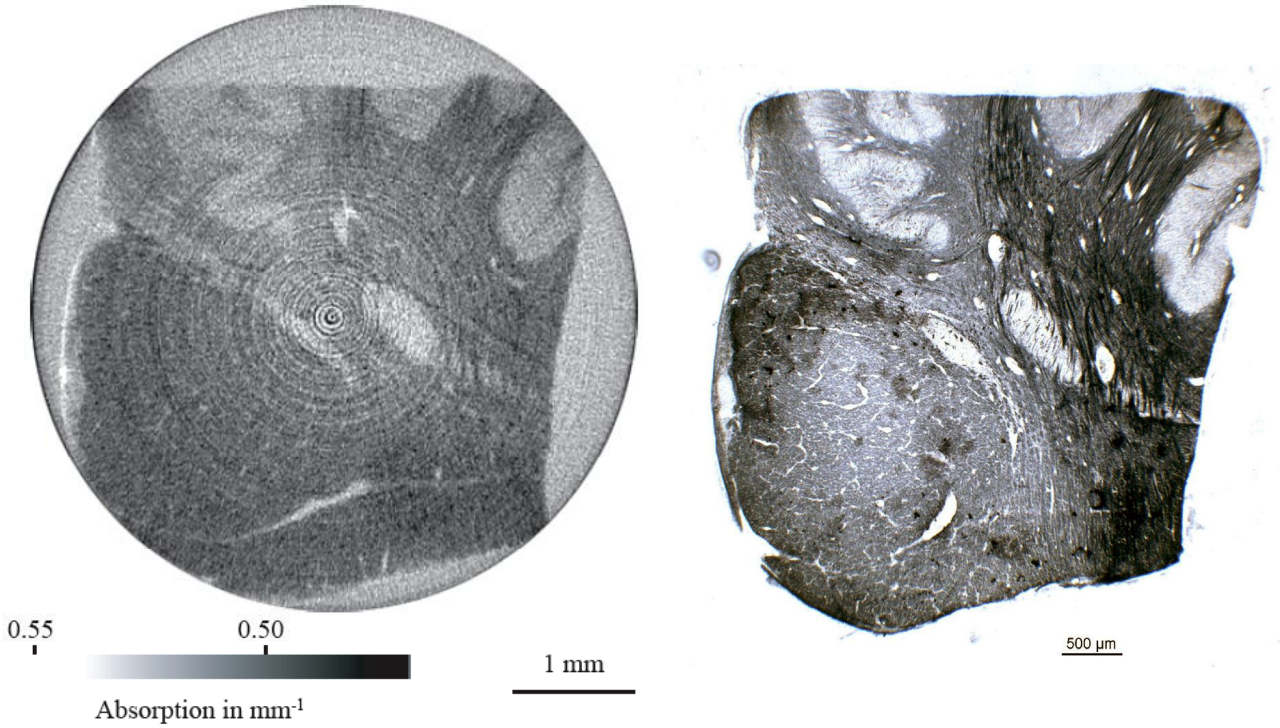

Fig. 6. Comparison of a typical SRμCT slice with the related myelin stained section of the medulla oblongata that shows similarities and differences of the results obtained. Several anatomical features can be detected in both images, whereby others are only visible in one of the images. The SRμCT slice and the myelin section are adjacent to the Nissl-stained sections shown in Fig. 2.

7. DISCUSSION

It is rather surprising that non-stained soft tissue such as brain measured in phosphate buffer environment gives rise to a reasonable absorption contrast. Such contrast allows the segmentation of the specimen's morphology (outer shape) and inner structures including blood vessels and agglomerates of neuronal cells (nuclei) without any kind of cutting artifact. The comparison of the huge amount of SRμCT slices with the restricted number of histological ones enables the labeling of features and, even more important, the quantification of artifacts and tissue distortions. The quantification of the distortions requires a 2D-3D registration algorithm that leads to a unique solution.

We expect that phase-contrast SRμCT leads to much better density resolution (contrast), which has to be proven experimentally. Preliminary experiments by the use of the grating interferometer,[12] however, show only marginal improvements so far. The detailed analysis is ongoing and will be published elsewhere.[13]

The complex structures of the medulla with its fine blood vessels is well resolved in the tomograms of the paraffin embedded specimens but not in the ones of the brain in phosphate buffer also because of the limited spatial resolution of 5.7 µm. The holes with diameters of several 10 µm in the histological slices are attributed to the larger blood vessels. These blood vessels are collapsed in the 3D configuration, probably as the result of slight press in the Eppendorf container, and presumably originate significant distortions in the histological slices.

The value of the tomograms is the possibility to non-rigidly register the different sets of stained histological slices in order to generate the 3D representation of parts of the brain anatomy.

The combination of the different morphological information on the true micrometer scale belongs to promising tools to reach the next level of improvement of the Morel atlas, which serves as anatomical basis for different minimally or non-invasive surgical procedures.

ACKNOWLEDGMENT

The experiments were carried out in the frame of the approved proposal I-04-077 (HASYLAB at DESY). The authors gratefully acknowledge the support of the staff at the beamline especially Felix Beckmann (GKSS Research Center) during the data acquisition and reconstruction.

REFERENCES

1. A. Morel, M. Magnin, D. Jeanmonod, J. Comp. Neurol. 387, 588-630 (1997).
2. K. Niemann, V. Mennicken, D. Jeanmonod, et al., Neuroimage 12, 601-616 (2000).
3. R.H. Davies, C.J. Twining, T.F. Cootes, et al., IEEE TMI 21, 525-537 (2002).
4. M.A. Styner, K.T. Rajamani, L.P. Nolte, et al., Proc. IPMI'03, 63-75 (2003).
5. M. Germann, A. Morel, F. Beckmann, B. Müller: Three-dimensional characterization of brain tissue using synchrotron-radiation-based micro computed tomography, Annual Report HASYLAB, pp. 1079-1080 (2005).
6. L. Grodzins, Nucl. Instrum. Meth. 206, 541- (1983).
7. B. Müller, P. Thurner, F. Beckmann, et al., in Developments of X-ray tomography III, edited by U. Bonse (SPIE- The International Society for Optical Engineering, San Diego, USA), Vol. 4503, 178-188 (2001).
8. F. Beckmann, in Developments in X-ray Tomography III, edited by U. Bonse (SPIE - The International Society for Optical Engineering, San Diego, USA), Vol. 4503, 34 (2001).
9. A.C. Kak and M. Slaney, *Principles of Computerized Tomographic Imaging*, Society of Industrial and Applied Mathematics, 2001.
10. P. Thurner, F. Beckmann, B. Müller, Nucl. Instrum. Meth. B 225, 599-603 (2004).
11. G. Schaltenbrand, W. Wahren, *Atlas for Stereotaxy of the Human Brain.* Stuttgart: Thieme, 1977.
12. T. Weitkamp et al. SPIE Proc. Vol. 6318 (2006).
13. F. Pfeiffer, O. Bunk, C. Kottler, C. David, P. Cloetens, M. Germann, A. Morel, B. Müller in preparation.